# Accuracy and convergence properties of the extended linear APW method

E.E. Krasovskii†

*Institute of Metal Physics National Academy of Sciences of Ukraine, Vernadskogo 36, 252680, Kiev-142, Ukraine*



A detailed analysis of the accuracy of linear augmented plane wave (LAPW) methods is presented. A number of known APW-like formalisms is reviewed, and their properties are related to the flexibility of the radial basis set used for the augmentation. The accuracy of the wavefunctions produced by the standard LAPW and by the extended LAPW method (ELAPW) is numerically tested using Nb metal as an example. It is shown that the methods employing an extended set of radial basis functions yield better accuracy and acquire convergence properties similar to those of Slater's APW. In contrast to the previous analyses of the accuracy of linear methods we take into account the matching constraints at the muffin-tin sphere and focus on the problem of fitting the radial function to an exact solution with a different logarithmic derivative. Based on this approach we deduce a value which characterizes the closeness of the linear APW-like method to Slater's APW. A possibility to further improve presently used extended LAPW techniques is discussed.

## I. INTRODUCTION

The direct variational methods to calculate the one-electron Bloch states in crystals are divided with regard to the eigenvalue dependence of the basis set into nonlinear methods, e.g. the KKR[1] and the APW,[2] and linear methods, of which the most widely used are the LMTO[3,4] and the APW-like schemes.[3,5–12] The former approach requires that the trial function pointwise satisfy the Schrödinger equation inside the so-called muffin-tin spheres, whereas in the linear methods it is a linear combination of a number of spherical waves. The nonlinear methods are precise in the sense that they allow the eigenenergies and wavefunctions to be determined with unlimited accuracy. However, they lead to a nonlinear eigenvalue problem, and, in general, produce wavefunctions with a discontinuity in slope at the sphere boundary. Besides this, in the case that the potential inside the muffin-tin spheres is not spherically symmetric additional programming effort is required to construct the exact solution in the spheres.

The above shortcomings have been avoided in the linear methods, which employ an eigenvalue-independent basis set. There the wavefunction is by construction continuous with continuous derivative everywhere in the unit cell. Another advantage of using the fixed basis set is that the formalism is easily extended to the case of a potential of general shape.[13]

In Slater's APW[2] for a given crystal potential the trial function is a Bloch function defined by its plane wave expansion in the interstitial as well as by the eigenvalue in question, $E_{\boldsymbol{k}\lambda}$, the only constraint imposed on the function being its continuity at the sphere boundary. Hence the function inside the spheres is not uniquely determined by its shape in the interstitial, and the function in the two regions can be varied (to some extent) independently of each other. We shall refer to this property of the basis set as flexibility. The situation is different in rigid linear methods, such as Andersen's LAPW,[3] where once the energy parameters of the method have been chosen the function inside the spheres is uniquely determined by the plane wave expansion in the interstitial region.

It has been shown[14] that it is the lack of flexibility that prevents the usual LAPW[3] from producing accurate wavefunctions even if the eigenvalue is within a few eV from the energy parameters of the method. To construct a flexible function within a linear method, i.e., to return the variational freedom cancelled by the requirement of continuity in slope, one must use an extended radial basis set (more than two radial functions for each angular momentum). The first linearization of the APW method was the modified APW (MAPW) presented in 1970 by Bross.[9] In spite of its advantage of being flexible this method has not been widely used, and the majority of the APW calculations have been based on the LAPW formalism developed five years later by Andersen[3].

In the '90s the growing requirements to the accuracy of band-structure calculations brought the flexible methods into wider use; the extended versions of the LAPW have been applied to the calculation of the total energy[11] and the excited states,[12] and a considerable gain in accuracy over the usual LAPW has been reported. Recently an extended version of the LMTO has been presented.[4] In this work we use the ELAPW method described in Ref. 15.

Apart from its efficiency in the bulk band-structure calculations the ELAPW has been found to be well suited for treating the semi-infinite solid, where the evanescent solutions of the Schrödinger equation must be included. It has been shown[15] that the extension of the radial basis set makes it possible to apply a $\mathbf{k}\cdot\mathbf{p}$ formulation of the ELAPW without considerable loss of accuracy, which in turn allows the analytical continuation of the matrix equation to the complex $\boldsymbol{k}$-space.

The aim of this paper is to elucidate the source of the error in the linear methods and to suggest the ways of improving their accuracy. There exists a variety of the APW schemes, which employ different prescriptions for the radial basis functions. We show that the convergence properties of the APW-like methods are primarily determined by the degree of the flexibility of the radial basis set, while the shape of individual basis functions is of secondary importance. Existing APW schemes are compared and classified in Sec. II.

Andersen[3] originally suggested that the accuracy of the linear methods can be understood in terms of the quality of the parametrization of the logarithmic derivative function $D(E)$. This approach is justified insofar as the wavefunction is atomic-like, however, in the general case the matching conditions at the sphere should be taken into account. The parametrization curves are considered in Sec. III, where it is indicated that inclusion of the matching conditions strongly changes the shape of the curves.

In considering the accuracy of a linear method it is usually implied that the function inside the sphere is matched to a high-quality wavefunction in the interstitial. In Sec. IV, we give up this assumption and focus on the ability of the radial basis set to reproduce the exact solution with a different rather than with the same logarithmic derivative. In that section a quantity is introduced which expresses the closeness of the linear method to Slater's APW. In Sec. V the wavefunctions in the unit cell are numerically tested. It is shown that, contrary to popular belief, in the linear method the wavefunctions cannot be improved by mere increasing the number of plane waves, even though the energy parameters are chosen close to the band energy of interest.

## II. THE APW-LIKE FORMALISMS

In a variational method the wavefunction is sought as a linear combination of $N$ basis functions

$$\Psi_{\boldsymbol{k}\lambda}(\boldsymbol{r}) = \sum_{i=1}^{N} C_i(\boldsymbol{k},\lambda)\psi_i(\boldsymbol{k},\boldsymbol{r}). \tag{1}$$

Here $\boldsymbol{k}$ is a Bloch vector, $\lambda$ is a band number, and $C_i$ are the variational coefficients. In the APW-like methods the trial function in the interstitial region is a finite sum of plane waves

$$\Psi_{\boldsymbol{k}\lambda}(\boldsymbol{r}) = \sum_{\boldsymbol{G}}^{N_G} t_{\boldsymbol{G}}(\boldsymbol{k},\lambda)\exp(i\boldsymbol{K}\boldsymbol{r}), \tag{2}$$
$$\boldsymbol{K} = \boldsymbol{k} + \boldsymbol{G},$$

where $\boldsymbol{G}$ is the reciprocal lattice vector; $N_{\boldsymbol{G}} \leq N$.

Without loss of generality any APW-like basis set can be thought of as consisting of $N_{\boldsymbol{G}}$ APWs and $N - N_{\boldsymbol{G}}$ localized orbitals[11,12]

$$\Psi_{\boldsymbol{k}\lambda}(\boldsymbol{r}) = \sum_{\boldsymbol{G}} t_{\boldsymbol{G}}(\boldsymbol{k},\lambda)\psi(\boldsymbol{K},\boldsymbol{r}) + \\ + \sum_{nlm} q_{nlm}(\boldsymbol{k},\lambda) z_{nl}(r) Y_{lm}(\hat{\boldsymbol{r}}). \tag{3}$$

(We consider the case of a single muffin-tin sphere per unit cell). The APWs are derived from the plane waves by replacing the Bessel functions $j_l(Kr)$ in the Rayleigh decomposition of the plane wave inside the sphere with radial functions $u_l(K,r)$, which match the Bessel functions in value (and, in linear methods, in slope) at the sphere radius. Inside the sphere located at $\boldsymbol{r}$=0 the APW reads

$$\psi(\boldsymbol{K},\boldsymbol{r}) = \sum_{lm} A_{lm}(\hat{\boldsymbol{K}}) u_l(K,r) Y_{lm}(\hat{\boldsymbol{r}}), \tag{4}$$

$$A_{lm}(\hat{\boldsymbol{K}}) = 4\pi i^l Y^*_{lm}(\hat{\boldsymbol{K}}). \tag{5}$$

The localized functions, $z_{nl}$, vanish in the interstitial and have both zero value and zero slope at the sphere.

We now define the angular momentum decomposition of the variationally obtained wavefunction inside the sphere

$$\Psi_{\boldsymbol{k}\lambda}(\boldsymbol{r}) = \sum_{lm} \chi_{lm}(r) Y_{lm}(\hat{\boldsymbol{r}}), \qquad r \leq S.$$

Here $\chi_{lm}$ are the radial parts of the spherical waves, $S$ is the sphere radius. The further discussion will be restricted to the case of a spherically symmetric potential inside the sphere. Then the $\chi_{lm}$ must be $m$-independent solutions of the radial Schrödinger equation $\chi_{lm}(r) = \phi_l(E_{\boldsymbol{k}\lambda}, r)$, $E_{\boldsymbol{k}\lambda}$ being the eigenenergy. This is the case in Slater's APW, but not in the linear methods, where $\chi_{lm}$ are, in general, $m$-dependent and may strongly deviate from $\phi_l(E_{\boldsymbol{k}\lambda}, r)$.

Depending on the choice of $u_l$ the basis set can be referred to as eigenvalue-adjusted (Slater's APW), potential-adjusted (the majority of the presently used linear methods), or potential-independent. Within the potential-independent approach two schemes are known: the pure plane-wave expansion, used in the pseudopotential calculations, and the spline APW,[10] where a set of localized spline functions is added to the plane waves. The spline APW calculations clearly demonstrate the importance of making the basis set flexible: in spite of the fact that none of the radial functions involved resemble solutions of the radial Schrödinger equation the method yields accurate wavefunctions over a wide energy interval from the deeply lying core states up to high-energy free-electron-like states.[10]

Still, the potential-adjusted methods have certain advantages. First, the evaluation of the matrix elements of the hamiltonian or momentum operators is much simpler in this case. Secondly, if one is interested in a moderately wide energy interval, say, from the semi-core states (1-2 Ry below the Fermi level) up to the excited states involved in the ultraviolet photoemission measurements (2-3 Ry above the $E_F$), the number of additional functions, $N - N_{\boldsymbol{G}}$, can be greatly reduced.

In the potential-adjusted methods both $u_l$ and $z_{nl}$ are linear combinations of a number of solutions of the radial Schrödinger equation, $\phi_{\nu l}(E_{\nu l}, r)$,

$$\hat{H}_r \phi_{\nu l}(E_{\nu l}, r) = E_{\nu l} \phi_{\nu l}(E_{\nu l}, r),$$

and their energy derivatives, $\dot{\phi}_{\nu l}(E_{\nu l}, r)$,

$$(\hat{H}_r - E_{\nu l}) \dot{\phi}_{\nu l}(E_{\nu l}, r) = \phi_{\nu l}(E_{\nu l}, r),$$

$$< \dot{\phi}_{\nu l} \mid \phi_{\nu l} >= 0.$$

$E_{\nu l}$ are called energy parameters of the method. Let $N_s$ and $N_d$ be respectively the number of the radial solutions and energy derivatives used to construct the APWs and localized orbitals. Of this set only two functions for each $l$ are needed to match an APW in both value and slope at the sphere. The others are included either to extend the APW set (flexible methods,[9,11,15] $N > N_{\boldsymbol{G}}$) or to improve the APWs, i.e., to bring them in advance closer to the solutions to be obtained (rigid methods,[5,7,8] $N = N_{\boldsymbol{G}}$).

The differences in the representation of the radial part in various APW-like methods are summarized in Table I. Though all the methods except for Slater's APW lead to a linear matrix eigenvalue problem, in what follows the term linear methods is used only for the potential-adjusted methods.

Let $\Phi_l(K, r)$ be the linear combination of two radial functions that matches the Bessel function, $j_l(Kr)$, both in value and in slope at the sphere radius. For the rigid methods we can write (variable $\boldsymbol{r}$ is dropped)

$$\chi_{lm} = u_{lm}(\{t_{\boldsymbol{G}}\}, \{E_{\nu l}\}) \equiv \sum_{\boldsymbol{G}} t_{\boldsymbol{G}} A_{lm}(\hat{\boldsymbol{K}}) \Phi_l(K),$$

and for the flexible methods it is

$$\chi_{lm} = u_{lm}(\{t_{\boldsymbol{G}}\}, \{E_{\nu l}\}) + \sum_n q_{nlm}(\boldsymbol{k}, \lambda) z_{nl}.$$

The simplest version of a rigid LAPW[3,6] ($N_s = N_d = 1$) has been adopted in the majority of studies, and more sophisticated rigid schemes[5,7,8] did not show any noticeable advantage over it. Various prescriptions to construct the spherical waves are summarized in Table II.

## III. THE STANDARD LAPW

Consider the case $N_s + N_d = 2$ in more detail. Here, to within a factor, the function $\Phi(K)$ is determined by its radial logarithmic derivative, $D$. We shall use the notation $\Phi(D) = \Phi(K)/\sqrt{< \Phi(K) \mid \Phi(K) >}$.

It is convenient to have two orthogonal radial functions, which can be achieved either by using two solutions having the same logarithmic derivative or (as suggested by Marcus[16]) by using a solution, $\phi_\nu$, and its energy derivative, $\dot{\phi}_\nu$. The former choice was implemented in the alternative APW (AAPW).[5] The distance between the energy expectation values of the functions is very large in this case (more than 1 Ry), therefore the variational method is expected to suppress the contribution of one of the functions in the vicinity of the other energy parameter, thereby reducing the variational freedom. The latter choice is devoid of this shortcoming: $\phi_\nu$ and $\dot{\phi}_\nu$ have the same energy expectation value, $E_\nu$.

The quality of the radial set is usually estimated by comparing the exact energy dependence of the radial logarithmic derivative,

$$D^{true}(E) = S\frac{\phi_l'(E,r)}{\phi_l(E,r)}\bigg|_S, \tag{6}$$

to the parametrization curve

$$E_{par}(D) =< \Phi_l(D) \mid \hat{H}_r \mid \Phi_l(D) > . \tag{7}$$

The exact curve has a cotangent-like shape, the branches being referred to by the main quantum number. The energy $E_{nl}$ at which the logarithmic derivative, $D^{true}$, equals $-l-1$ is called the center of the $n$-th band. The slope of the parametrization curves changes sign twice at $D = D_+$ and $D = D_-$,

$$D_\pm = D_{\dot{\nu}} + S^{-1}\left(\phi_\nu(S)\dot{\phi}_\nu(S) \pm \frac{\dot{\phi}_\nu^2(S)}{\sqrt{< \dot{\phi}_\nu \mid \dot{\phi}_\nu >}}\right)^{-1}, \tag{8}$$

$$D_{\dot{\nu}} = S\frac{\dot{\phi}_\nu'(r)}{\dot{\phi}_\nu(r)}\bigg|_S .$$

The asymptote of the curve $E_{par}(D)$ is at

$$E_a = E_\nu - \frac{\phi_\nu(S)/\dot{\phi}_\nu(S)}{1+ < \dot{\phi}_{\nu l} \mid \dot{\phi}_{\nu l} > \phi_\nu^2(S)/\dot{\phi}_\nu^2(S)}. \tag{9}$$

In the vicinity of $D_{\nu l} \equiv D^{true}(E_\nu)$ the variational estimate (7) is correct to $o(E-E_\nu)^3$.[3,6] Depending on the position of $E_\nu$ relative to the asymptotes of the true curve, the parametrization curve adopts one of three possible shapes (see Fig. 1). For the $n$-th branch ($n > 1$) two energies, $E_d < E_u$, divide the branch into three intervals, the character of the parametrization curve being determined by which interval $E_\nu$ belongs to.

$$\begin{aligned} &Case\ 1, \quad E_\nu \geq E_u: \quad && D_{\dot{\nu}} \in [D_-, D_+], D_{\dot{\nu}} \geq D_\nu, \\ &case\ 2, \quad E_\nu \leq E_d: \quad && D_{\dot{\nu}} \in [D_-, D_+], D_{\dot{\nu}} < D_\nu, \\ &case\ 3, \quad E_d < E_\nu < E_u: \quad && D_{\dot{\nu}} \notin [D_-, D_+]. \end{aligned} \tag{10}$$

In the cases 1 and 2 the $E_{par}(D)$ curve extends to the $(n+1)$-st and $(n-1)$-st branch respectively; in both cases the corresponding asymptotes are properly described, and the interval of the unphysical behavior of the parametrization, where $\frac{dD}{dE} > 0$, is finite. In the third case the parametrization curve has negative slope only within a finite interval, and its asymptote is far from those of the true curve. In band-structure calculations the states in the vicinity of the asymptote are usually of physical interest, so case 3 is normally avoided.

An example for the $p$-orbitals in the muffin-tin sphere of Nb metal is shown in Fig.1. The centers of the semi-core $4p$-band and the free-electron-like $5p$-band are $E_{4p} = -2.3$ Ry and $E_{5p} = 1.5$ Ry (all energies are relative to the Fermi level). The $5p$-branch is separated by asymptotes at $-2.1$ and $4.1$ Ry; $E_d = -1.3$ Ry, and $E_u = 0.75$ Ry. Note, that the $E_{\nu 1}$ being chosen in the valence band region (from $-0.45$ Ry to $E_F = 0$) leads to case 3.

The functions $\phi_l(E)$ and $\Phi_l(D^{true}(E))$, whose energy expectation values have been compared in Fig. 1, are equally normalized but have different values at the sphere radius, $\phi_l(E,S) \neq \Phi_l(D^{true}(E),S)$. It is evident that to assess the quality of the radial function $\chi_{lm}(r)$ produced by the LAPW one should compare the function to the exact solution having not only the same logarithmic derivative but also the same value at the sphere. This point does not question the validity of the law $o(E-E_\nu)^3$, however, as far as the accuracy is concerned, the curves $E_{par}(D)$ are only reasonable in the close vicinity of $D_\nu$.

Let us lift the requirement of normalization (this constraint is artificial as it is not imposed by the LAPW formalism) and impose the matching constraint, which does exist in the LAPW. The result is depicted in Fig. 1 by the dot-dashed line, which shows the energy expectation value of the function $\Phi_l(D(E),r)\cdot\phi_l(E,S)/\Phi_l(D(E),S)$. It is seen that the energy range where the error of the radial function is small is considerably narrower than that suggested by the $E_{par}(D)$ curve.

It should be emphasized that the analysis in this section is pertinent to the accuracy of the method only if the correct logarithmic derivative, $D^{true}$, is generated by the variational procedure. Experience shows that except for atomic-like states this almost never occurs in practice (see Sec. V and Ref. 14).

## IV. ACCURACY OF THE WAVEFUNCTION INSIDE THE SPHERE

In this section we establish connection between the linear methods and Slater's APW, which remains the most precise technique and converges most rapidly.

In contrast to the linear methods, in the APW the $\chi_{lm}(r)$ does not in general continue analytically to the interstitial, where the angular momentum expansion reads

$$\begin{aligned}\Psi_{\boldsymbol{k}\lambda}(\boldsymbol{r}) &= \sum_{lm}\Theta_{lm}(r)Y_{lm}(\hat{\boldsymbol{r}}), \quad r>S,\\ \Theta_{lm}(r) &= \sum_{\boldsymbol{G}} t_{\boldsymbol{G}}A_{lm}(\hat{\boldsymbol{K}})j_l(Kr),\\ \chi_{lm}(S) &= \Theta_{lm}(S).\end{aligned} \tag{11}$$

Yet in the converged APW calculation the representations in the two regions match in slope to within the numerical accuracy, $\Theta'_{lm}(S)=\chi'_{lm}(S)$, and the well-converged wavefunction is the best possible. However, experience shows that even if the wavefunction is underconverged, the APW eigenvalues are more precise than those obtained with linear methods.

Let us look at the problem from the side of the interstitial region. We retain the coefficients $t_{\boldsymbol{G}}$ from the APW calculation and try to reproduce the APW result with a linear method, i.e., to construct the $\chi_{lm}$ as close as possible to $\phi_l(E_{\boldsymbol{k}\lambda})$.

First consider the problem of reproducing the exact wavefunction (here we can drop the subscript $m$). In this case we need to minimize the error

$$\delta_l(E) = \parallel \phi_l(E)-\chi_l \parallel \tag{12}$$

under two constraints

$$\chi_l(S)=\phi_l(E,S), \quad \chi'_l(S)=\phi'_l(E,S).$$

The solution, $\bar{\chi}_l$, is a projection of the function $\phi_l(E)$ onto a subspace formed by $N_s+N_d$ radial functions. The energy dependence of the error is determined by the choice of the energy parameters, $E_\nu$, and by the number of the radial functions.

The results for the $p$-orbitals in the muffin-tin sphere of the Nb metal are shown in Fig. 2. The energy interval covers the semi-core $4p$-states and the $5p$-branch. Five setups are considered. The first one (solid curve) is the LAPW setup as usually chosen to describe the unoccupied free-electron-like states: we use two functions, $\phi_\nu$ and $\dot{\phi}_\nu$, $E_\nu=E_{5p}$. Then we add the solution at the center of the semi-core band, $\phi_\mu$, $E_\mu=E_{4p}$ (dashed curve). In the third calculation (long-dashed curve) we use three functions as well, but now they are $\phi_\mu$, $\dot{\phi}_\mu$ and $\phi_\nu$. Then we extend the basis set to comprise four functions: $\phi_\nu$, $\dot{\phi}_\nu$, $\phi_\mu$, $\dot{\phi}_\mu$ and shift the $E_\nu$ to higher energies. Two curves are shown, for $E_\nu=2.8$ Ry (dotted curve), and for $E_\nu=5.3$ Ry (dot-dashed curve). The upper and the lower panels of Fig. 2 show the deviation of the function, $\delta(E)=\parallel\phi_l(E)-\bar{\chi}_l\parallel$, and the energy error, $\Delta E=<\bar{\chi}_l\mid\hat{H}_r\mid\bar{\chi}_l>-E$, respectively.

In the usual LAPW the deviation of the orbital from the exact solution grows rapidly with the distance from $E_\nu$, and the energy error in the valence-band region exceeds 0.1 Ry. With the choice $N_s=2$, $N_d=1$ the interval between $E_\mu$ and $E_\nu$ is described with a reasonable quality, but the accuracy deteriorates rapidly beyond this interval. It is interesting to note that using the energy derivative from the 'semi-core' branch yields better performance in the valence band region (long-dashed curve) than using the one from the $5p$-branch, which the valence band belongs to (dashed curve).

Including the fourth function diminishes the errors by an order of magnitude, and even when the $E_\nu$ is pushed far into the $6p$-band, the function and the energy deviations remain tolerable. It should be also noted that the curves are much smoother in this case, so the distortions in the band structure due to the errors in the representation of the orbitals are expected to be less pronounced.

Now consider an underconverged APW calculation. The error of the eigenvalue, $E = E_{\boldsymbol{k}\lambda}$, is negligible, but there is a kink at the sphere: $\phi_l'(E,S) \neq \Theta_l'(S)$. Again we retain the APW result for the plane-wave expansion, $\{t_{\boldsymbol{G}}\}$, and try to fit the linear combination $\chi_l$ to the solution $\phi_l(E)$. Now the logarithmic derivatives of two functions differ, $D_{\boldsymbol{k}\lambda} \neq D^{true}(E)$. We use the notation

$$D_{\boldsymbol{k}\lambda} \equiv S \frac{\Theta_l'(r)}{\Theta_l(r)}\bigg|_S . \tag{13}$$

The deviation of the orbital is a function of two variables

$$\delta(E,\Delta D) = \| \phi_l(E) - \bar{\chi}_l(D_{\boldsymbol{k}\lambda}) \|, \tag{14}$$

$$\Delta D = D^{true}(E) - D_{\boldsymbol{k}\lambda}.$$

The $\Delta D$ dependence has a simple form

$$\delta(E,\Delta D) = \sqrt{A^2(E)\Delta D^2 + B(E)\Delta D + C(E)}. \tag{15}$$

Experience shows that the first term dominates even for moderately large $\Delta D$, especially when the number of functions is large. (With increasing the number of radial functions the minimum of the curve $\delta(E,\Delta D)$ decreases much faster than the coefficient $A(E)$). To elucidate the meaning of the coefficient $A(E)$ let us perform a linear transformation of the radial set to obtain $N_s + N_d$ functions, $u$, $v$, and $z_i$, $1 \leq i \leq N_s + N_d - 2$, such that

$$\begin{aligned} u(S) = 0, \quad & u'(S) = 1/S, \\ v(S) = 1, \quad & v'(S) = 0, \\ z_i(S) = 0, \quad & z_i'(S) = 0, \\ < u \mid z_i > = & < v \mid z_i > = 0. \end{aligned}$$

Then $A(E)$ is easily expressed as

$$A(E) = \phi_l(E,S)\sqrt{< u \mid u >}. \tag{16}$$

The larger is the number of functions $z_i$ the smaller is $\| u \|$ and the more flexible is the basis set. Obviously the expansion of $u$ in terms of $z_i$ does not converge uniformly, and we always have $\| u \| \neq 0$; however, by extending the radial basis set we can approach Slater's APW as closely as necessary.

It is because of large values of $A(E)$ in the rigid methods that the accuracy cannot be improved by placing the $E_\nu$'s close to the $E_{\boldsymbol{k}\lambda}$ without having a well-converged function in the interstitial. On the other hand, reliable results can be obtained with a flexible method even if the plane-wave expansion is far from exact. In practice, the plane-wave expansion is always underconverged, hence the measure of the closeness of the linear method to Slater's APW is given by the value $\| u \|$.

Each new function ($\phi$ or $\dot{\phi}$) added to the radial basis set diminishes the value $A(E)$ by a factor of about two or three. Thus even a moderate extension of the basis set is very efficient. This has been demonstrated by the ELAPW calculation of the orthorhombic $Al_3Ni$ (four formula units per unit cell).[17] There we have found the valence band energies to converge much faster in the ELAPW than in the LAPW, which enabled us to achieve better accuracy with a smaller hamiltonian matrix.

Obviously the performance of the linear method is the better the closer the energy parameters are to the energy interval of interest. However, in practice, the $E_\nu$'s cannot be chosen too close to each other because then the radial basis set becomes numerically linearly dependent, and computational instabilities in the matrix eigenvalue problem may occur. The Gram determinant of the $N_s + N_d$ normalized functions decreases rapidly if the $E_\nu$'s are brought closer to each other than 4-5 Ry. The effect becomes more pronounced if the set does not contain pairs of orthogonal functions (i.e., if $N_d = 0$). Thus from the practical standpoint the ELAPW ($N_s = N_d = 2$) has an advantage over the MAPW ($N_s = 4, N_d = 0$) because with the basis sets yielding comparable accuracy the determinants in the ELAPW are two orders of magnitude larger than in the MAPW.

## V. NUMERICAL TESTS OF ACCURACY

To estimate the quality of the variationally obtained wavefunction we compare its energy expectation value in the interstitial region

$$E_{out}(\boldsymbol{k},\lambda) = \frac{\int\limits_{out} \Psi^*_{\boldsymbol{k}\lambda}\hat{H}\Psi_{\boldsymbol{k}\lambda}d\boldsymbol{r}}{\int\limits_{out} \Psi^*_{\boldsymbol{k}\lambda}\Psi_{\boldsymbol{k}\lambda}d\boldsymbol{r}} \tag{17}$$

with the eigenvalue, $E_{\boldsymbol{k}\lambda}$. Here the integration is over the interstitial region. The two values coincide if the function is exact, hence deviation of the well-converged value of $E_{out}(\boldsymbol{k},\lambda)$ from the band energy is a measure of quality of the wavefunction.[14]

In Fig. 3 we compare LAPW ($N_s = N_d = 1$) and ELAPW ($N_s = N_d = 2$) calculations. The first set of parameters was the same in both methods: $E_{\nu 0} = E_{5s}$, $E_{\nu 1} = E_{5p}$, $E_{\nu 2} = E_{4d}$, and the parameters for higher $l$ were at $E = 0.3$ Ry. In the ELAPW the additional functions for $l \leq 3$ were included, their energy parameters being $\sim 10$ Ry above the $E_{\boldsymbol{F}}$. Five energy levels are shown, $\lambda$ =1, 3, 7, 9, and 10 for the $\boldsymbol{k}$-point N of the *bcc* Nb. The levels are ordered with respect to the energy, $E_{\boldsymbol{k}\lambda}$; the numbering starts in the valence band.

For these electron states the extension does not affect eigenvalues; the difference between the LAPW and ELAPW energies is less then 3 mRy. It is seen that, in contrast to Slater's APW, the values $E_{out}(\boldsymbol{k},\lambda)$ do not converge to the eigenvalue. It is interesting to note that the rate of convergence in the ELAPW is the same as in the LAPW, but in the ELAPW the converged local expectation values are closer to the eigenvalue than in the LAPW.

The largest difference observed in the ELAPW calculation is for $\lambda = 3$. This is a state of almost pure $p$-character (50% $p$ + 3% $f$), and it occurs far from the center of the $5p$ branch, $E_{\boldsymbol{k}3} = 0.17$ Ry ($E_{5p} = 1.5$ Ry). The difference cannot be reduced by including $4p$-orbitals instead of the $6p$-orbitals (circles in Fig. 3). The conclusion is that the orbital in question cannot be properly reproduced by a linear combination of remote orbitals. This is presumably due to the close neighborhood of the critical point: the function $D^{true}(E)$ changes sign at $E = 0.5$ Ry. The upper states, $\lambda$=7, 9, 10, have a considerable contribution of $f$-character. In the LAPW the accuracy is seen to deteriorate rapidly with the distance from $E_{\nu 3} = 0.3$ Ry. In some instances a high-quality wavefunction in the interstitial can be obtained with a limited number of APWs, and the error is solely due to the representation of the function $\chi_{lm}(r)$. For example, when we choose $E_{\nu 1} = E_{\boldsymbol{k}3}$ the difference between $E_{out}(\lambda = 3)$ and $E_{\boldsymbol{k}3}$ vanishes.

To assess the quality of the functions $\chi_{lm}(r)$ we calculate the resultant logarithmic derivative, $D_{\boldsymbol{k}\lambda}$, (see Eq.(13)) and determine the energy of the exact solution having this logarithmic derivative, $\tilde{E}(D_{\boldsymbol{k}\lambda})$,

$$D^{true}(\tilde{E}(D_{\boldsymbol{k}\lambda})) = D_{\boldsymbol{k}\lambda}. \tag{18}$$

The deviation of $\tilde{E}(D_{\boldsymbol{k}\lambda})$ from $E_{\boldsymbol{k}\lambda}$ is a measure of the quality of the variationally obtained orbital.[14] To avoid the problem of $m$-dependence we apply this test only to $s$-orbitals. The results for $\lambda$=8 (39% $s$ + 47% $d$) are shown in Fig. 4. The eigenvalue, $E_{\boldsymbol{k}8} = 0.91$ Ry, is within the range of validity of Andersen's parametrization (7) both for $s$- and for $d$-orbitals: $E_{5s} = 0.23$ Ry and $E_{4d} = 0.18$ Ry. Again, with an increasing number of the plane waves, $\tilde{E}(D_{\boldsymbol{k}\lambda})$ does not converge to $E_{\boldsymbol{k}\lambda}$, however, with the extension switched on the error reduces by 30%. We pay special attention to the fact that the deviation of the energy of the variationally obtained $s$-orbital from the band energy is 50 mRy though the linear parametrization is correct to 1 mRy in this energy region.

The state $\lambda$=8 provides an example of the situation when the well-converged wavefunction is far from exact. With $E_{\nu l} = E_{\boldsymbol{k}8}$ for all $l$ the difference $E_{\boldsymbol{k}8} - E_{out}(\lambda = 8)$ converges to 60 mRy in the LAPW and to 115 mRy in the ELAPW (the eigenvalues calculated by the two methods coincide). In this case the linear methods are prevented from producing a correct wavefunction by the orthogonality conditions. A variationally obtained wavefunction is an eigenvector of a matrix problem, and, consequently, it is orthogonal to other eigenvectors, which may be rather rough (e.g. as a result of their eigenvalues being far from the energy parameters). The requirement of being orthogonal to inaccurate functions spoils the wavefunction in question.

## VI. CONCLUSIONS

Rigid schemes are aimed at accurate description of the radial solution over a given energy interval. The logarithmic derivative parametrization developed by Andersen seems to be the most elegant and efficient. Yet it should be noted that no matter how accurate is the description, in the APW-like methods we, in general, cannot take advantage of it, because even if the eigenvalue is well within the energy interval where the exact radial solution is perfectly reproduced, the variational method normally produces wavefunctions with logarithmic derivatives far from their true values. As a result we obtain perfectly parametrized radial functions, which are infinitely close to solutions of the radial Schrödinger equation, though for an energy which is far from the eigenvalue in question.

This is an unavoidable shortcoming of rigid methods, where the logarithmic derivatives are uniquely determined by the coefficients of the plane wave expansion in the interstitial, the plane wave expansion being normally far from accurate even if it is well-converged.

It should also be emphasized that well-converged wavefunctions scarcely appear in practical calculations, especially when the crystal structure is open and there are many inequivalent atoms in the unit cell. In such cases it is important to be able to describe the wavefunction in the vicinity of nuclei as precisely as possible having a rather rough description in the interstitial. Experience with Slater's APW shows that this aim can be achieved, and that an underconverged plane-wave expansion can coexist with reliable functions inside the spheres. This property of the non-linear APW is taken up by extended linear methods, the continuity in slope at the sphere boundaries being an important improvement over Slater's scheme. The closeness of the linear method to Slater's APW is related to the flexibility of the basis set and it can be quantitatively expressed by Eq.(16).

Slater's APW is flexible only within the family of solutions of the radial Schrödinger equation, whereas the extended radial basis set can be used to simulate any function. This feature makes it possible to apply a $\mathbf{k}\cdot\mathbf{p}$ formulation of the ELAPW without considerable loss of accuracy.

In the rigid LAPW schemes the accuracy can be improved by including more plane waves only if the energy parameters are close to the eigenvalue in question. If this is not the case, the well-converged wavefunction may remain inaccurate. The analytical expression of the single-sphere formalism cannot be used to estimate the error of the linear method, however we have shown that simple calculations can be performed in advance to visualize the properties of the basis set and to chose the number and the location of the energy parameters.

The performance of the ELAPW is not strongly dependent upon the choice of the energy parameters, therefore reliable wavefunctions over a wide energy interval can be obtained with a fixed set of energy parameters. This property has been exploited in the band-structure calculations where it is necessary to obtain the wavefunctions of semi-core states, valence band, and free-electron-like states as orthogonal eigenvectors of a single matrix eigenvalue problem.

Extension of the radial basis set should be used with care, as the functions may appear to be linearly dependent to within the numerical accuracy. The further improvement of the ELAPW method would be to use an orthogonal potential-adjusted basis set, which would lift the restrictions on the choice of the energy parameters. This cannot be done by straightforward orthogonalization of the set of radial solutions and their energy derivatives, because the determinant of their overlap matrix being small would strongly emphasize the numerical errors of the radial functions. This problem has been avoided in the spline APW, although at the expense of the radial set being potential-independent.

The ELAPW method used in the present paper is a considerable improvement over Andersen's original version of the LAPW, however, it seems to be not the optimal method for the band-structure calculations. The optimal method requires a different prescription for the radial basis functions, which would lift the problem of linear dependence and minimize the value $\| u \|$ (Eqs.(15 - 16)) for a given number of radial basis functions.

## ACKNOWLEDGMENT

I am grateful to Dr. D. Singh for a critical reading of the manuscript and encouraging comments. I wish to thank F. Starrost for stimulating discussions and valuable suggestions. I am indebted to Professor Dr. W. Schattke and Professor Dr. V.N. Antonov for their continuous support. I wish to thank Dr. O.V. Krasovska for computational and programming assistance.

This work was completed during my research visit to the Christian-Albrechts-Universität of Kiel supported by a grant of the Deutsche Forschungsgemeinschaft.

† Present Address: Institut für Theoretische Physik, Christian-Albrechts-Universität, Leibnizstrasse 15, D-24118 Kiel, Germany.

[1] J. Korringa, Physica **13**, 392 (1947); W. Kohn and N. Rostoker, Phys. Rev. **94**, 1111 (1954).
[2] J.C. Slater, Phys. Rev. **51**, 846 (1937).
[3] O.K. Andersen, Phys. Rev. B **12**, 3060 (1975).

[4] F. Aryasetiawan, O. Gunnarsson, Phys. Rev. B **49**, 7219 (1994).
[5] D.D. Koelling, Phys. Rev. B **2**, 290 (1970).
[6] D.D. Koelling and G.O. Arbman, J. Phys. F **5**, 2041 (1975).
[7] T. Takeda and J. Kubler, J. Phys. F **9**, 661 (1979).
[8] D.J. Shaughnessy, G.R. Evans, M.I. Darby, J. Phys. F **17**, 1671 (1987).
[9] H. Bross, G. Bohn, G. Meister, W. Schubö, H. Stöhr, Phys. Rev. B **2**, 3098 (1970).
[10] H. Bross and G.M. Fehrenbach, Z. Phys. B **81**, 233 (1990).
[11] D. Singh, Phys. Rev. B **43**, 6388 (1991); D.J. Singh, *Planewaves, Pseudopotentials and the LAPW Method*, (Kluwer, Boston 1994).
[12] E.E. Krasovskii, A.N. Yaresko, V.N. Antonov, J. Electron Spectrosc. Relat. Phenom. **68**, 157 (1994).
[13] E. Wimmer, H. Krakauer, M. Weinert, and A.J. Freeman, Phys. Rev. B **24**, 864 (1981).
[14] E.E. Krasovskii, V.V. Nemoshkalenko, V.N. Antonov, Z. Phys. B **91**, 463 (1993).
[15] E.E. Krasovskii, W. Schattke, Solid State Commun. **93**, 775 (1995).
[16] P.M. Marcus, Int. J. Quantum. Chem. Suppl. **1**, 567 (1967).
[17] G. Cubiotti, E.E. Krasovskii, O.V. Slobodyan, Yu.N. Kucherenko, V.N. Antonov, J. Phys: Condens. Matter **7**, 4865 (1995); G. Cubiotti, A.D. Laine, G. Mondio, E.E. Krasovskii, O.V. Krasovska, Yu.N. Kucherenko, V.N. Antonov, Yu.V. Kudryavtsev, V.G. Ivanchenko, J. Phys: Condens. Matter **8**, 2549 (1996).

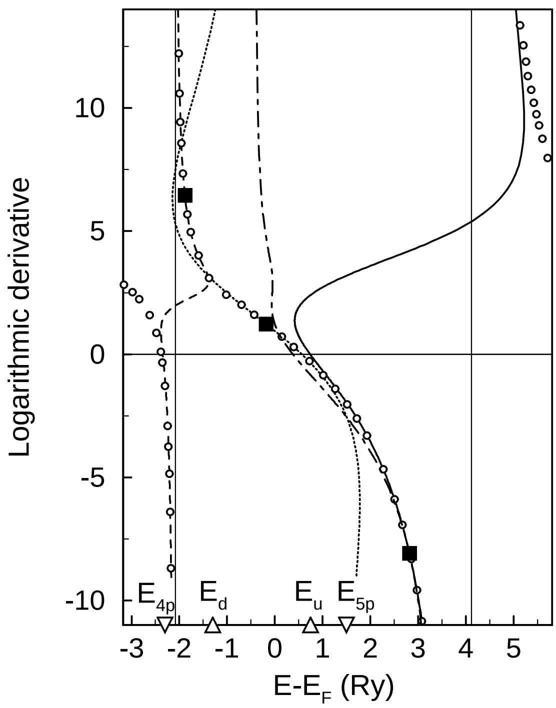


FIG. 1. Behavior of the parametrization curve, $E_{par}(D)$, (see Eq.(7)) depending on the location of the energy parameter. The exact curve, $D^{true}(E)$, is shown by open circles. The squares denote location of the parameters for the cases 1, 2, and 3, (see Eq. (10)) shown by solid, dashed, and dotted line respectively. The dot-dashed line shows the logarithmic derivative dependence of the energy expectation value of the radial function normalized so as to match the exact solution in both value and slope at the sphere.

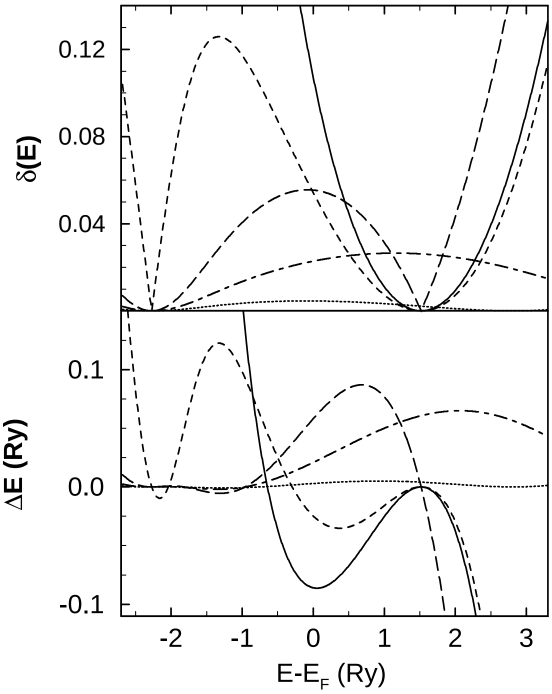


FIG. 2. Energy dependence of the error in representation of the exact radial solution (see Eq. (12)) by a linear combination of $N_s$ fixed solutions and $N_d$ energy derivatives (upper panel) and the energy error (lower panel). $N_s = N_d = 1$ (solid line), $N_s = 2$, $N_d = 1$ (dashed and long-dashed lines), $N_s = N_d = 2$ (dotted and long-dashed lines).

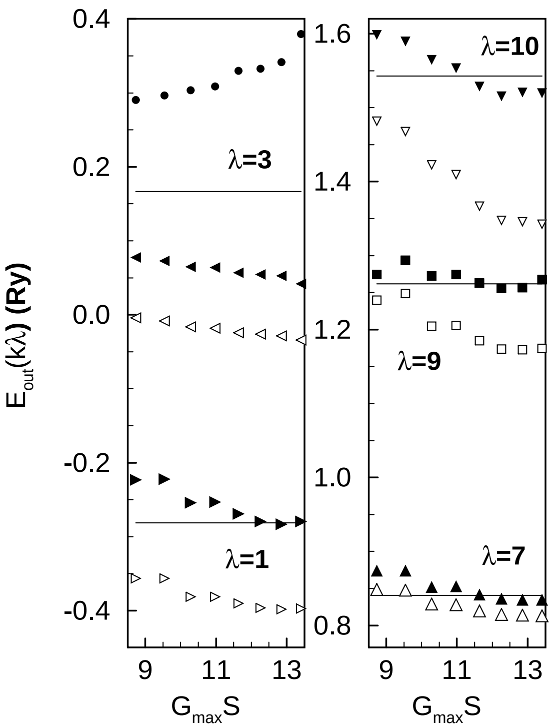


FIG. 3. Convergence of the energy expectation value in the interstitial (see Eq. (17)) for several energy levels in the $\boldsymbol{k}$-point N of the *bcc* Nb in LAPW (open symbols) and ELAPW (solid symbols). Horizontal lines show the eigenvalues.

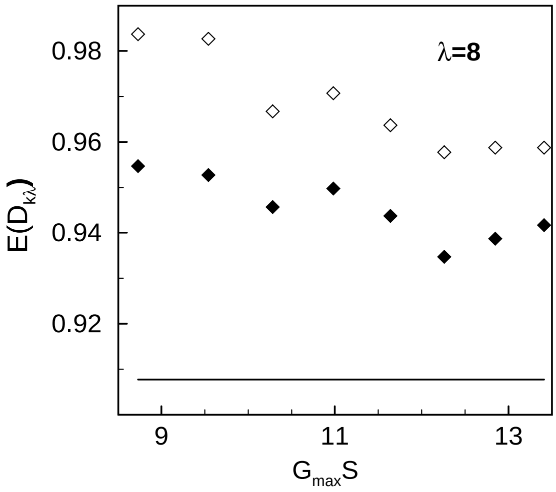


FIG. 4. Convergence of the logarithmic derivative, $D_{\boldsymbol{k}\lambda}$, of the $s$-orbital in the angular-momentum decomposition of the variationally obtained wavefunction. Energies $E(D)$ are shown at which $D^{true}(E(D)) = D$. The LAPW results are shown by open diamonds, and the ELAPW results by solid diamonds. Horizontal line denotes the eigenvalue. The LAPW values coincide very closely with the energy expectation values of the normalized $\chi_{00}$ function. In the ELAPW the orbital is not uniquely determined by the $D_{\boldsymbol{k}\lambda}$ and its energy is much closer to the eigenvalue than the value $\tilde{E}(D_{\boldsymbol{k}\lambda})$.

TABLE I. Representation of the radial part of the $l$-th spherical wave inside the muffin-tin sphere in different APW-like methods. Choice of the representation determines the continuity of the wavefunction and the completeness of the set. The basis sets of the linear methods are incomplete in the sense that there always exists a Bloch solution that cannot be represented by the infinite number of the energy-independent APWs. On the other hand, all APW sets are overcomplete in the sense that the representation of a Bloch function by the infinite number of APWs is not unique.

| Method | $\chi_{lm}(r)$ | $\frac{d^n}{dr^n}\chi_{lm}(r)\Big\vert_S$ continuity | completeness |
|---|---|---|---|
| Slater's APW | $\phi_l(E_{\boldsymbol{k}\lambda}, r)$ | $n_{max} = 0$ | overcomplete |
| linear methods | $\sum_{\nu=1}^{N_s} a_{\nu lm}\phi_{\nu l}(r) + \sum_{\nu=1}^{N_d} b_{\nu lm}\dot{\phi}_{\nu l}(r)$ | $n_{max} \le N_s + N_d - 1$ | incomplete |
| spline APW | $\sum_{i=1}^{N_G} t_i A_{ilm} j_l(K_i r) + \sum_{\nu=1}^{N_{spline}} s_{\nu lm}(r)$ | $n_{max} = 1$ | overcomplete |
| plane waves | $\sum_{i=1}^{N_G} t_i A_{ilm} j_l(K_i r)$ | $n_{max} = \infty$ | complete |

TABLE II. Comparison description of the linear methods employing potential-adjusted radial basis set. Rigid and flexible methods are shown in upper and lower panels respectively.

| Method | $N_s$ | $N_d$ | $\frac{d^n}{dr^n}\chi_{lm}(r)\Big\vert_S$ continuity | Additional constraints on $\Phi_l(K, r)$ |
|---|---|---|---|---|
| AAPW[5] | $\ge 2$ | 0 | $n_{max} = 1$ | $\delta\langle\Phi \mid H - E \mid \Phi\rangle = 0$ |
| LAPW-75[3,6] | 1 | 1 | $n_{max} = 1$ | |
| LAPW-79[7] | $\ge 2$ | 0 | $n_{max} = N_s - 1$ | |
| LAPW-87[8] | 3 | 0 | $n_{max} = 1$ | $\Phi(h(K)) = \sum_{k=0}^{2} \frac{h^k}{k!} R_k$ |
| MAPW[9] | $\ge 2$ | 0 | $n_{max} = 1$ | |
| LAPW+LO[11] | $\ge 2$ | $\ge 1$ | $n_{max} = 1$ | |
| ELAPW[12] | $\ge 2$ | $N_d = N_s$ | $n_{max} = 1$ | |